Polymerase manager protein UmuD directly regulates *Escherichia coli* DNA polymerase III α binding to ssDNA

Kathy R. Chaurasiya[1], Clarissa Ruslie[1], Michelle C. Silva[2], Lukas Voortman[2], Philip Nevin[2], Samer Lone[1,3], Penny J. Beuning[2,*] and Mark C. Williams[1,*]

[1]Department of Physics, Northeastern University, Boston, MA 02115, USA, [2]Department of Chemistry and Chemical Biology, Northeastern University, Boston, MA 02115, USA and [3]Department of Chemical Sciences, Bridgewater State University, Bridgewater, MA 02325, USA

ABSTRACT

Replication by *Escherichia coli* DNA polymerase III is disrupted on encountering DNA damage. Consequently, specialized Y-family DNA polymerases are used to bypass DNA damage. The protein UmuD is extensively involved in modulating cellular responses to DNA damage and may play a role in DNA polymerase exchange for damage tolerance. In the absence of DNA, UmuD interacts with the α subunit of DNA polymerase III at two distinct binding sites, one of which is adjacent to the single-stranded DNA-binding site of α. Here, we use single molecule DNA stretching experiments to demonstrate that UmuD specifically inhibits binding of α to ssDNA. We predict using molecular modeling that UmuD residues D91 and G92 are involved in this interaction and demonstrate that mutation of these residues disrupts the interaction. Our results suggest that competition between UmuD and ssDNA for α binding is a new mechanism for polymerase exchange.

INTRODUCTION

DNA polymerase III (DNA pol III) holoenzyme is a 10-subunit protein complex that efficiently and accurately replicates the entire genome of *Escherichia coli* (1,2). It is composed of three subassemblies: the polymerase core, the β processivity clamp and the clamp loader complex. Polymerase and proofreading activities are conducted by the core sub-assembly, which consists of the polymerase subunit α, the proofreading subunit ε and the θ subunit, which has a role in stabilizing the core (3,4). The β processivity clamp encircles the DNA and provides a platform for the polymerase core to bind, providing α with access to the primer-template and facilitating processive replication. The clamp loader complex, which consists of the γ, δ, δ′, τ, χ and ψ subunits, loads the β clamp onto the DNA (5) with τ tethering the polymerase core to the replisome (6), and coordinating simultaneous replication of the leading and lagging strands of the replication fork (6,7).

Although DNA pol III efficiently replicates undamaged DNA, replication is disrupted upon encountering damaged bases (8–11). Formation of a RecA filament on accumulated single-stranded DNA (ssDNA) triggers the SOS response (12), resulting in the upregulation of genes encoding numerous proteins involved in DNA damage repair and tolerance (13). These proteins include the potentially mutagenic Y-family polymerases DNA pol IV (DinB) and DNA pol V (UmuD′$_2$C) (14–16). Replication of damaged DNA can proceed once DNA pol III α is replaced with one of these Y-family polymerases, which can replicate damaged DNA in a process known as translesion synthesis (17–20). DNA pol V is composed of two subunits, the cleaved form of UmuD and the UmuC polymerase. DNA polymerase manager protein UmuD regulates the cellular response to DNA damage in part, along with UmuC, by decreasing the rate of replication, thereby allowing time for non-mutagenic DNA repair processes to occur (21–23). UmuD undergoes a RecA/ssDNA-facilitated auto-cleavage of 24 amino acids of its N-terminal 'arms' to form UmuD′. UmuD forms a tight dimer (UmuD$_2$), which is the predominant form for the first 20–40 min of the SOS response after which the cleaved form UmuD′ is the predominant species (22,24). Although UmuD and UmuD′ are expected to be dimeric under all the conditions studied here (25) for

*To whom correspondence should be addressed. Tel: +1 617 373 7323; Fax: +1 617 373 2943; Email: mark@neu.edu
Correspondence may also be addressed to Penny J. Beuning. Tel: 617 373 2865; Fax: 617 373 8795; Email: penny@neu.edu
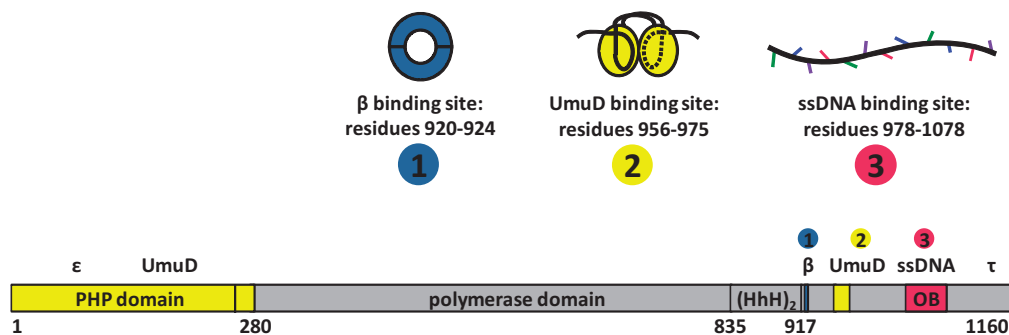
Figure 1. Diagram of DNA pol III α, with domain labels within the boxes and known interaction sites above the boxes (sequence numbering shown below). The two UmuD binding sites, one in the N-terminal domain and one in the C-terminal domain of α, are shown in yellow (29). The CTD binding site (residues 956–975) is adjacent to the β clamp binding site (residues 920–924, shown in blue) (30), and recent biochemical experiments show that UmuD displaces α from the β clamp (29). This UmuD binding site is also adjacent to the OB fold (red), where ssDNA binds α (31), an observation that led us to hypothesize that UmuD also inhibits α binding to ssDNA.

simplicity, we will refer to these dimeric forms as UmuD rather than $UmuD_2$ and UmuD′ rather than $UmuD'_2$, respectively. UmuD also regulates mutagenesis in the cell through its interaction with the Y-family DNA polymerase DinB, by inhibiting DinB-dependent −1 frameshift mutagenesis, and with UmuC (14,26,27).

UmuD interacts with several components of DNA pol III, including the polymerase subunit α, the β clamp and the proofreading subunit ε (28). Recent ensemble biochemical experiments have shown that there are two UmuD-binding sites on the α subunit, one in the N-terminal domain and one in the C-terminal domain (29) (Figure 1). The C-terminal binding site (residues 956–975), which has higher affinity for full-length UmuD relative to the cleaved form UmuD′ (29), is adjacent to the β clamp binding site (residues 920–924) (30), which tethers the polymerase to its DNA template. UmuD, but not UmuD′, releases α from the β clamp, which may inhibit DNA replication and facilitate polymerase exchange (29). The C-terminal UmuD binding site of α is also adjacent to the OB-fold (residues 975–1160), through which α binds ssDNA (31), suggesting that UmuD may be competing with ssDNA for binding to α. We hypothesized that one way UmuD contributes to a DNA damage checkpoint is by disrupting the interaction between α and ssDNA, thereby inhibiting replication. To test this hypothesis, we have used single molecule DNA stretching to quantify α binding to ssDNA in the presence of wild-type UmuD and several UmuD variants designed from a computational docking analysis of the complex. We find that wild-type UmuD competitively inhibits α binding to ssDNA through UmuD-α interactions, whereas a single amino acid substitution, D91K in UmuD, disrupts this inhibition.

MATERIALS AND METHODS

Proteins and plasmids

Wild-type UmuD was expressed from the pSG5 plasmid in BL21 (DE3) (Novagen) as previously described (32,33). UmuD D91 and G92 were changed to lysine by site-directed mutagenesis of pSG5 using the QuikChange Kit (Agilent) and confirmed by sequencing the resulting

plasmids (Macrogen USA). Wild-type UmuD and all variants were purified as previously described (32).

Wild-type DNA pol III α was expressed from the pET28a-α plasmid in Tuner competent cells (Novagen) and purified using both a Nickel His-trap column (GE Healthcare) and a heparin column (GE Healthcare) as previously described (29). Fractions collected after the heparin column were diluted 6-fold with buffer HA [50 mM HEPES (pH 7.5); 1 M NaCl; 2 mM beta-mercaptoethanol; 20% glycerol] and loaded onto a hydroxyapaptite column (BioRad Bioscale Mini CHT Type 1, 5 ml, 40 μm cartridge) to concentrate the protein; protein concentrator devices were avoided because they significantly reduced the stability and activity of DNA pol III α. After washing with 10 column volumes of buffer HA, buffer HB [100 mM sodium phosphate (pH 6.5); 1 M NaCl; 2 mM beta-mercaptoethanol; 20% glycerol] was used to elute the protein from the column isocratically in 2 column volumes. Fractions containing DNA pol III α were dialyzed against protein storage buffer [50 mM HEPES (pH 7.5); 150 mM NaCl; and 50% glycerol] and stored at −20°C.

Single molecule DNA stretching

In DNA stretching experiments with optical tweezers, a single λ DNA molecule is captured between two polystyrene beads inside a flow cell. One bead is fixed on a micropipette tip, and the other is held in a dual-beam optical trap (34). As the fixed bead is extended at 100 nm/s, the tethered DNA molecule exerts a force on the trapped bead, which is measured by deflection of the trapping laser beams. The force on the DNA molecule is measured as a function of DNA extension. As the DNA is stretched, the double-stranded DNA (dsDNA) helix undergoes a force-induced melting transition into ssDNA (Figure 2A). The bases anneal on DNA release, exhibiting minimal hysteresis, or mismatch between the extension and release curves. After the DNA is stretched and released in buffer only [10 mM HEPES, 100 mM Na^+ (pH 7.5)], the solution in the flow cell is exchanged to include protein. Subsequent force-extension curves are obtained in the presence of α, UmuD, or both proteins.

Force-extension curves in the presence of 250 nM α alone exhibit significant hysteresis, as protein bound to the exposed ssDNA prohibits the two strands from annealing on DNA release. All single molecule experiments were performed by waiting at fixed extension for 30 min before DNA release, which has been established as a quantitative method of characterizing α binding to ssDNA (31). The fraction of ssDNA bound f_{ss} may be described in terms of observed length b (31):

$$b(F_{ss}) = b_{ds}(1 - f_{ss}) + b_{ss}f_{ss} \tag{1}$$

where b_{ds} as a function of force F is described by the Worm-Like Chain model:

$$b_{ds}(F) = B_{ds}\left[1 - \frac{1}{2}\left(\frac{k_B T}{P_{ds}F}\right)^{\frac{1}{2}} + \frac{F}{S_{ds}}\right] \tag{2}$$

with persistence length P_{ds}, end-to-end or contour length B_{ds} and stretch modulus S_{ds}. The Freely-Jointed Chain model describes the polymer elasticity of ssDNA:

$$b_{ss}(F) = B_{ss}\left[\coth\left(\frac{2P_{ss}F}{k_B T}\right) - \frac{1}{2}\frac{k_B T}{P_{ss}F}\right]\left[1 + \frac{F}{S_{ss}}\right] \tag{3}$$

The Worm-Like Chain and Freely-Jointed Chain polymer models shown in Figure 2 have typical parameter values [$B_{ds} = 0.34$ nm/bp, $P_{ds} = 48$ nm and $S_{ds} = 1200$ pN in Equation (2), $B_{ss} = 0.55$ nm/bp, $P_{ss} = 0.75$ nm, and $S_{ss} = 720$ pN in Equation (3)]. As previously described, the fits were confined to forces below 40 pN (31) to eliminate effects from changes in the force-extension curve of ssDNA due to protein binding.

These experiments were repeated in the presence of both α and UmuD, and the fraction of α-bound ssDNA f_{ss} as a function of UmuD concentration c_s was fit to a simple competitive DNA-binding isotherm:

$$f_{ss} = \left(1 - \frac{\frac{c_s}{K_d^{app}}}{1 + \frac{c_s}{K_d^{app}}}\right)f_{sat} \tag{4}$$

where K_d^{app} is the apparent equilibrium dissociation constant between UmuD and α in the presence of ssDNA, and f_{sat} is saturated α-ssDNA binding. A minor correction to added UmuD concentration c accounts for UmuD bound to α in solution; therefore, effective UmuD solution concentration c_s is (35):

$$c_s = \frac{c}{1 + K_a c_\alpha} \tag{5}$$

where $K_a = 9.1 \times 10^{-5}$ M^{-1} is the equilibrium association constant between UmuD and α in bulk solution (29) and the α concentration c_α is 250 nM.

Protein–protein docking

Protein–protein docking models were used to predict residues involved in the binding interaction between α and UmuD. The structures used for these docking models were a homology model of UmuD (33) and a homology model of full-length DNA pol III α (36). Protein complexes were predicted by docking DNA pol III α with UmuD using ClusPro 2.0 (37–40), GRAMM-X (41) and PatchDock (42). The top 10 results from each method were analyzed and compared. Local docking was performed using the RosettaDock server (43).

Thermal stability assay

A thermal stability assay was used to determine the melting temperature of UmuD variants relative to wild-type, as previously described (44). To determine whether mutations at positions D91 and G92 disrupt the stability of UmuD, melting temperatures of these variants were compared with those of wild-type. Samples containing
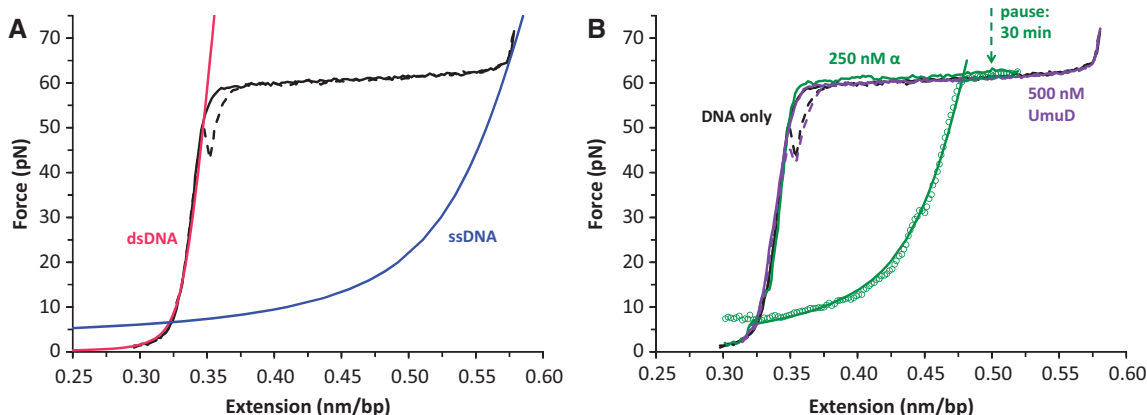

Figure 2. DNA pol III α binding to ssDNA characterized with single molecule force measurements. (**A**) Typical extension (solid black) and return (dashed black) of a single DNA molecule. The molecule undergoes a force-induced melting transition from dsDNA [red, Equation (2)] to ssDNA [blue, Equation (3)] at 62.6 ± 0.5 pN. (**B**) In the absence of protein (black), the DNA molecule anneals immediately on release, exhibiting minimal hysteresis, or mismatch between the stretch (solid) and release (dashed) curves. The force extension curves in the presence of 500 nM UmuD are the same within uncertainty as those of DNA only (purple), which shows that UmuD does not measurably bind DNA. In the presence of 250 nM α (green), pausing at a fixed DNA extension (dashed arrow) after the melting transition exposes ssDNA to α for 30 min, as previously described (31). On DNA release, α remains bound to the ssDNA (open circles), prohibiting the two strands from annealing. The DNA molecule is therefore a combination of dsDNA and protein-bound ssDNA, and fitting the release curve (open circles) to Equation (1) (solid line) yields the fraction of ssDNA bound to α ($f_{ss} = 0.58 \pm 0.02$).

20 μM of each variant in 50 mM HEPES (pH 7.5), 100 mM NaCl and 25× Sypro Orange (Invitrogen) were exposed to temperatures from 25°C to 80°C while monitoring the fluorescence emission intensity at 575 nm. Melting temperatures T_m were determined by taking the first derivative of the melting curves, as previously described (29).

RecA/ssDNA facilitated cleavage assay

Reactions were assembled as previously described (33) and incubated at 37°C for 45 min. After incubation, the cleaved product UmuD′ was separated from full-length UmuD using 18% SDS–PAGE. Bands were then analyzed using the image analysis software ImageQuant TL (Amersham Biosciences). Control reactions in the absence of RecA, ssDNA and adenosine-5′-3-thiotriphosphate γS were carried out to determine the amount of UmuD′ present due to spontaneous cleavage.

Tryptophan fluorescence assay

The equilibrium dissociation constants K_d between DNA pol III α and the UmuD variants were determined with a Varian Cary Eclipse Fluorescence Spectrophotometer, as previously described (29). DNA pol III α [5 μM in 50 mM HEPES (pH 7.5) and 100 mM NaCl] was titrated with varying volumes of 200–400 μM UmuD variants. Tryptophan fluorescence quenching was used to quantitate binding constants, as previously described (29).

RESULTS

UmuD inhibits α binding to ssDNA

In DNA stretching experiments, a single double-stranded λ-DNA molecule was captured between two polystyrene beads, one held in an optical trap and the other fixed on a micropipette tip. As the distance between the beads increases, measurements of the force on the DNA molecule yield a force-extension curve (Figure 2A, solid black line). At a constant force of 62.6 ± 0.5 pN, the dsDNA molecule undergoes a force-induced melting transition to ssDNA. This overstretching transition has been established as force-induced melting in the presence of DNA-binding proteins such as α, which is the case for the experiments presented in this work (34). When the tension on the DNA molecule is released (Figure 2A, dashed black line), the ssDNA generated by force anneals immediately into dsDNA, and the curve exhibits minimal hysteresis, or mismatch between DNA extension and release curves. The molecule is a well-characterized combination of dsDNA and ssDNA along the force-induced melting transition (45); therefore, waiting at constant extension for a fixed time exposes ssDNA to proteins in solution. The protein-bound ssDNA exhibits a change in observed length on DNA release, which is a direct measurement of protein binding to ssDNA. This single molecule technique has been established as a quantitative method of characterizing α–ssDNA binding (31). As expected, constant extension experiments in the presence of 250 nM α exhibit large hysteresis, indicating significant ssDNA binding (Figure 2B). Fits to Equation (1) yield the fraction of ssDNA bound by α, which agrees with previous results obtained by this method (31).

Introducing the DNA damage response protein UmuD disrupts the binding of α to ssDNA (Figure 3A). Constant extension experiments generate ssDNA for 30 min in the presence of both α and UmuD, and the fraction of ssDNA bound by α decreases with UmuD concentration. Control experiments demonstrate that UmuD does not bind DNA, as force extension curves in the presence of UmuD are the same within uncertainty as those of DNA only (Figure 2B, purple). Therefore, the interaction between UmuD and α inhibits α binding to ssDNA. A simple DNA-binding isotherm [Equation (4)] fit to the fraction of α bound as a function of effective UmuD concentration in solution
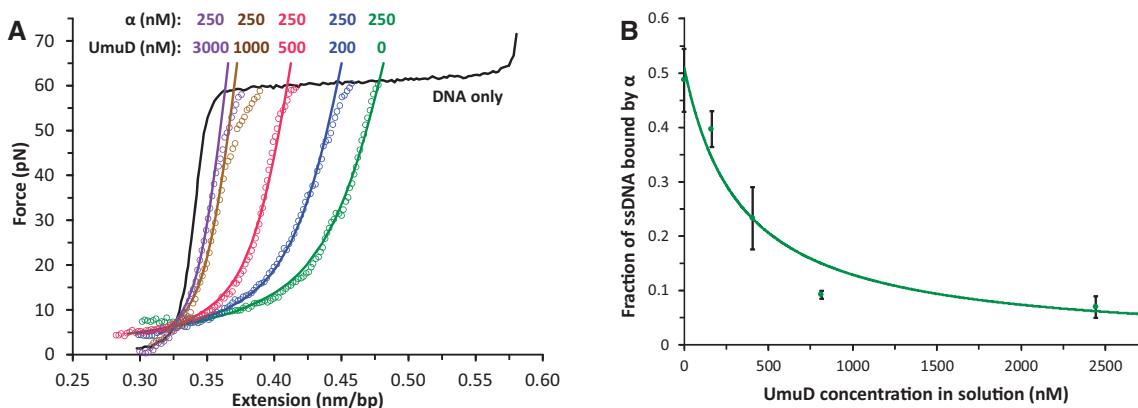

Figure 3. The fraction of ssDNA bound by α decreases with increasing UmuD concentration. (**A**) Force extension (solid black line) and release (open circles) curves for DNA in the absence (black) and presence of α and UmuD (open circles). Open circles are data points, and solid color lines are fits to Equation (1), which yield the fraction of ssDNA bound to α at each UmuD concentration. Fractions shown in these representative curves are 0.58 ± 0.02 in the absence of UmuD (green), 0.44 ± 0.02 at 200 nM UmuD (blue), 0.27 ± 0.02 at 500 nM UmuD (red), 0.09 ± 0.01 at 1 μM UmuD (brown) and 0.06 ± 0.01 at 3 μM UmuD (purple). (**B**) Fraction of ssDNA bound by α as a function of effective UmuD concentration in solution [Equation (5)]. Error bars represent standard error ($N \geq 3$) for all points except 2.5 μM, which represents propagated error. The solid line is a χ^2 fit to a simple DNA-binding isotherm [Equation (4)] that yields apparent equilibrium dissociation constant $K_d^{app} = 340 \pm 103$ nM between UmuD and α in the presence of ssDNA, and a saturated α-ssDNA binding fraction ($f_{sat} = 0.51 \pm 0.05$) consistent with previous single molecule results (31).

yields the apparent equilibrium dissociation constant $K_d^{app} = 340 \pm 103\,nM$ between UmuD and α in the presence of ssDNA (Figure 3B).

Specific UmuD variants disrupt the UmuD-α interaction

To predict potential α binding sites on UmuD, we used three global protein–protein docking methods. All three methods predicted an ensemble of complexes with UmuD binding near the N-terminal domain and C-terminal domain of DNA pol III α, consistent with the two previously characterized UmuD binding sites (29). At the C-terminal domain, a number of docking models suggested the formation of a salt bridge (Figure 4A) between the arginine residue of DNA pol III α at position 1068 (Figure 4B) and the aspartic acid residue of UmuD at position 91 (Figure 4C). As a result, UmuD residues D91, along with its adjacent neutral residue G92, were each mutated to lysine to disrupt this salt bridge (Figure 4C). We did not construct corresponding mutants in DNA pol III α at position 1068 because such a mutant would likely disrupt DNA binding as well.

To verify that the mutations did not destabilize UmuD, the melting temperatures of each UmuD variant were determined (Figure 5A). UmuD has two melting transitions, which have been assigned to the dissociation of the arms from the globular domain (see drawing in Figure 5A) and the melting of the globular domain, respectively (46). Both melting transitions of the UmuD variants are comparable with those of wild-type UmuD, indicating that the variants are properly folded. To test the effect of each mutation on the cleavage activity of UmuD, a RecA/ssDNA-facilitated UmuD cleavage assay was also performed. All variants were able to cleave efficiently to form the cleavage product UmuD' (Figure 5B); therefore, these mutations do not alter UmuD enzymatic activity. Because UmuD can undergo spontaneous cleavage, control reactions where RecA/ssDNA was not added to the UmuD variants were also carried out. The amount of UmuD' present in both the control reactions and the reactions with RecA/ssDNA was quantified separately to distinguish the amount of UmuD' produced only in the RecA/ssDNA-facilitated reaction (Figure 5B). Thus, the UmuD variants constructed show similar stability and similar RecA-ssDNA-faciliated cleavage efficiency as wild-type UmuD.

As shown in Figure 6, in the absence of DNA, the UmuD variant D91K disrupted the DNA pol III α-UmuD interaction by a 15-fold increase in K_d ($18 \pm 1.7\,\mu M$, compared with $1.1 \pm 0.6\,\mu M$ for wild-type UmuD), whereas no change was seen with the adjacent UmuD variant G92K ($K_d = 1.3 \pm 0.5\,\mu M$). When both positions were changed to lysine, D91K-G92K, a similar effect of decreased binding to α was observed ($K_d = 33 \pm 9.6\,\mu M$), confirming this position as a binding site for DNA pol III α. Although it is initially surprising that an adjacent residue mutation does not also disrupt UmuD-α interactions, unlike D91, we predict that a side chain at 92 would be angled away from the surface of UmuD (Figure 4A); therefore, it is less likely to participate directly in the interaction.
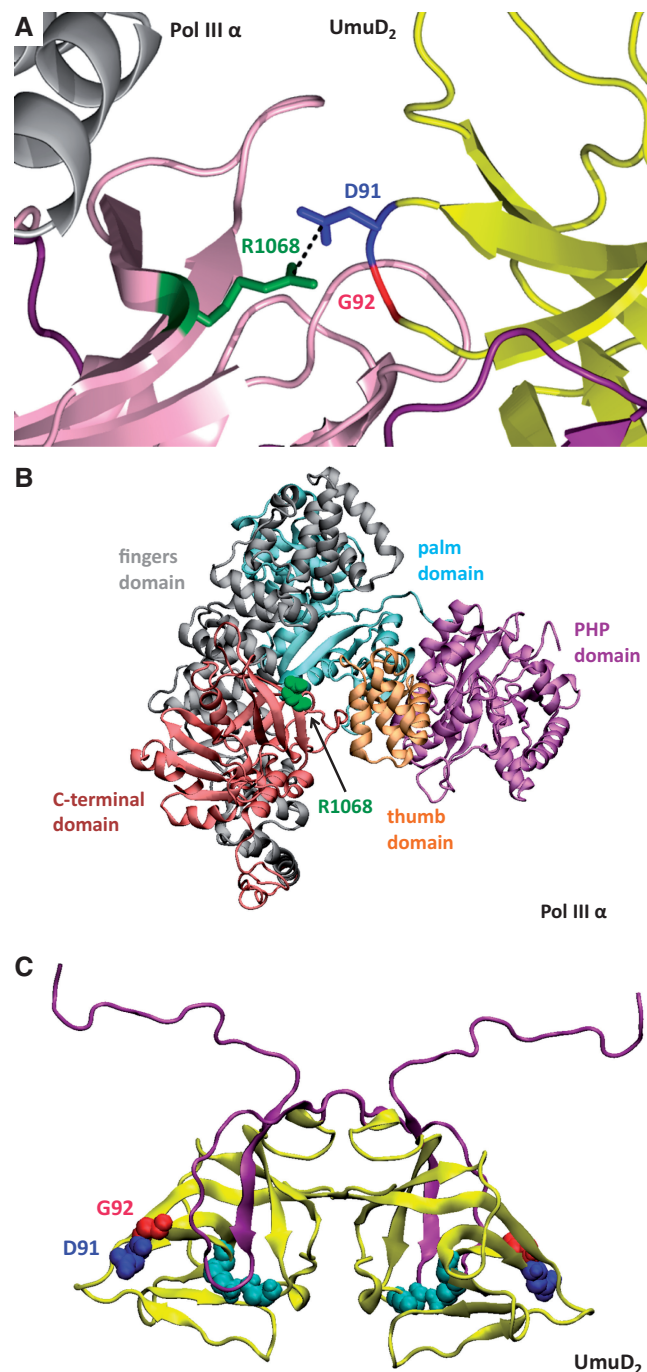

Figure 4. Docking model predicts residues involved in the interaction between DNA pol III α and UmuD. (**A**) The docking model predicts a salt bridge between the C-terminal domain of DNA pol III α (pink) and UmuD (yellow) at α residue R1068 (green) and UmuD residue D91 (blue). UmuD residue G92 (red) may also be involved in this interaction. (**B**) The homology model of α (36) showing arginine residue R1068 (green). The C-terminal domain (residues 917–1160) containing the binding sites for the β clamp, UmuD and ssDNA is shown in pink. (**C**) The homology model of full-length UmuD (33) showing the residues D91 (blue) and G92 (red) predicted to bind to DNA pol III α by protein–protein docking studies. The arms of UmuD are shown here in a 'trans' conformation where the arm of one monomer (both arms shown in purple) is bound to the globular domain of the other monomer (both globular domains shown in yellow). The active site residues S60 and K97 (cyan) cleave the N-terminal arms (residues 1–24) to form UmuD'.
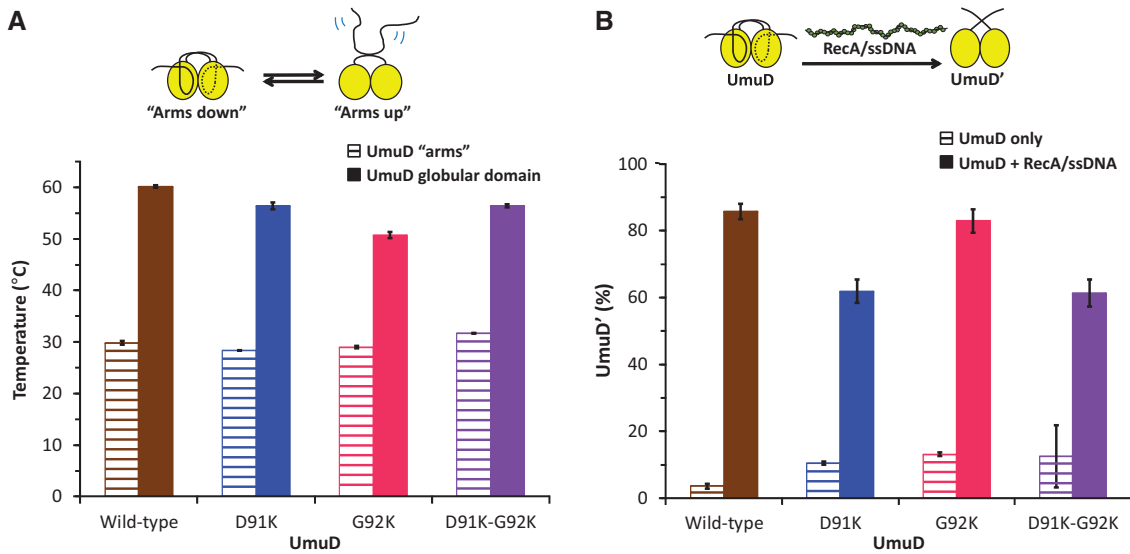
Figure 5. UmuD variants are structurally stable and enzymatically active. (**A**) Melting temperatures of all UmuD variants. The N-terminal 'arms' dissociate from the globular domain (drawing above) in the first transition (dashed), and the globular domain melts in the second transition (solid). (**B**) Relative amount of UmuD' produced by each variant in the RecA/ssDNA-facilitated self-cleavage reaction (45 min at 37°C, drawing above), in the absence (dashed) and presence (solid) of RecA/ssDNA. Thermal stability and self-cleavage activity of all variants is similar to wild-type UmuD, suggesting that the mutations had minimal impact on protein stability and function. Error bars represent standard error ($N \geq 3$).
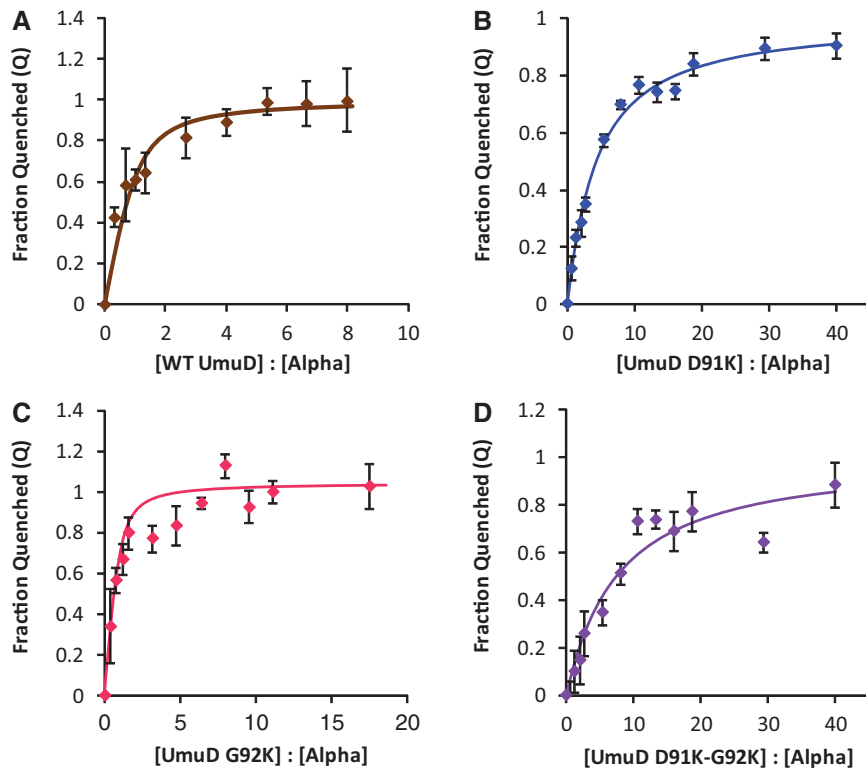

Figure 6. Binding curves between pol III α and UmuD variants measured by tryptophan fluorescence quenching. (**A**) The equilibrium dissociation constant K_d is $1.1 \pm 0.6 \mu M$ (29). (**B**) Binding to α is compromised by the D91K ($K_d = 18.1 \pm 1.7 \mu M$) mutation relative to wild-type UmuD. (**C**) The G92K variant ($K_d = 1.3 \pm 0.5 \mu M$) binds α with nearly the same affinity as wild-type UmuD. (**D**) In contrast, the binding affinity of the D91K-G92K variant ($K_d = 32.5 \pm 9.6 \mu M$) is significantly weaker than that of the D91K variant. This suggests that both the D91 and G92 residues are involved in the interaction of UmuD and α. Error bars indicate standard error ($N \geq 3$).
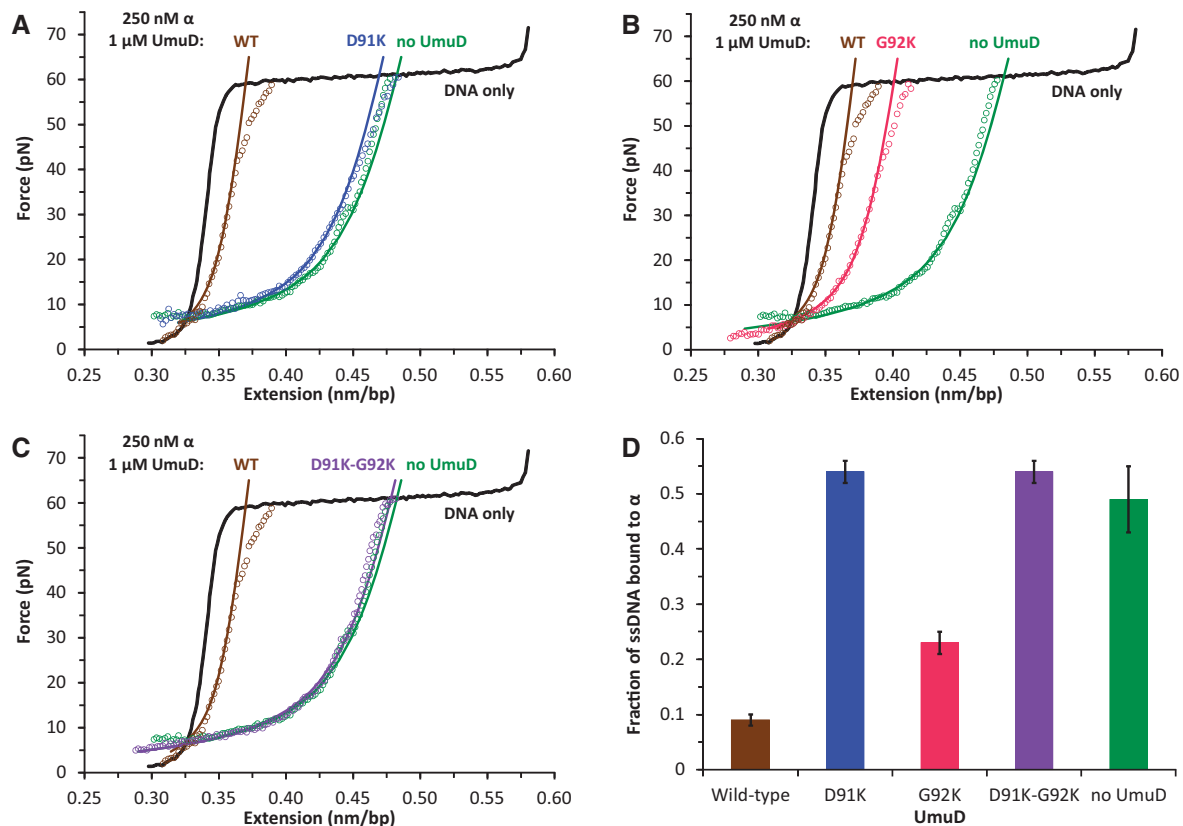
Figure 7. UmuD variants have compromised ability to disrupt α binding to ssDNA. (**A–C**) Force extension (solid black line) and release (open circles) curves for DNA in the absence (black) and presence of protein (open circles). Open circles are data points, and solid color lines are fits to [Equation (1)], which yield the fraction of ssDNA bound by α. (A) The fraction of α-bound ssDNA in the presence of 1 μM UmuD D91K (blue, 0.54 ± 0.02) is similar to that of α alone (green). The D91K variant lost the ability to inhibit α-ssDNA binding relative to wild-type UmuD (brown), which indicates that the D91 residue is required for the interaction between α and UmuD that disrupts α binding to ssDNA. (B) The G92K variant (red, 0.23 ± 0.02) partially retains its ability to disrupt the interaction between α and ssDNA. (C) The D91K-G92K mutation (purple) fully abolishes the ability of UmuD to disrupt α-ssDNA binding, and fraction of ssDNA bound to α is the same without the UmuD variant (0.58 ± 0.02). (**D**) Fraction of ssDNA bound to α in the presence of 1 μM UmuD variants. These single molecule results indicate that UmuD residue D91 is essential for the interaction between UmuD and α that disrupts α binding to ssDNA, but G92 is also involved in the interaction.

Specific variants disrupt UmuD inhibition of α binding to ssDNA

We used single molecule DNA stretching experiments to test whether the three UmuD variants retain the ability to disrupt binding between α and ssDNA. We previously showed using this single molecule method that α possesses two distinct DNA-binding activities: the $(HhH)_2$ domain binds dsDNA, whereas the C-terminal domain containing the OB-fold domain binds ssDNA (31). This method allows us to probe specifically the binding of α to ssDNA without the potential complications of DNA secondary structure or dsDNA binding. The biochemical results show that the D91K mutation compromises the ability of UmuD to bind α, and single molecule experiments demonstrate that the fraction of ssDNA bound by α in the presence of 1 μM UmuD D91K is only slightly smaller than that of α alone (Figure 7A). UmuD G92K has an affinity for α similar to that of wild-type UmuD, and DNA stretching shows that this variant retains most of its ability to inhibit α binding to ssDNA (Figure 7B). However, the double mutation D91K G92K yields a UmuD variant whose binding to α is dramatically

weakened and is completely unable to disrupt α-ssDNA binding (Figure 7C). UmuD residue D91 is therefore required for UmuD to bind α and disrupt its binding to ssDNA. Residue G92 also participates in the interactions that are responsible for UmuD inhibition of α-ssDNA binding. Collectively, these results show that these direct interactions between UmuD and α are responsible for the ability of UmuD to inhibit α binding to ssDNA.

DISCUSSION

In this work, we used a single-molecule method to demonstrate that UmuD inhibits the binding of α to ssDNA through its interaction with α. The apparent equilibrium dissociation constant K_d^{app} between UmuD and α is 340 ± 103 nM in the presence of ssDNA, which is similar to a previous measurement of the equilibrium dissociation constant between α and UmuD ($K_d = 1.1 ± 0.6$ μM) determined by using a tryptophan fluorescence binding assay in the absence of DNA. The reasonable agreement between apparent binding affinity and direct binding affinity implies that direct UmuD interactions with α are

responsible for ssDNA-binding inhibition. In addition, the measured apparent binding affinity between α and UmuD is within the range of cellular UmuD concentrations, suggesting that this interaction plays an important role in regulating α activity *in vivo* (47).

In addition to directly demonstrating that UmuD inhibits α binding to ssDNA, we used protein–protein docking models to identify potential UmuD–α interaction sites. The resulting models predicted that binding between UmuD and α involves UmuD residues D91 and G92 and α residue R1068. Biochemical experiments confirmed that the corresponding UmuD variants exhibit a compromised ability to bind α, despite the fact that the variants were demonstrated to be thermally stable and active for cleavage. Single-molecule experiments showed that the D91K variant completely fails to disrupt the α–ssDNA interaction, whereas the G92K variant only partially inhibits the ability of α to bind ssDNA. These results demonstrate that a direct α-UmuD interaction at these residues is responsible for UmuD inhibition of α–ssDNA binding. Another UmuD variant at position 91, D91A, has been shown to disrupt the UmuD–DinB interaction (26), suggesting the existence of a general binding site for polymerases on UmuD. In addition, peptide mapping experiments show that this region of UmuD provides a binding site for the protease ClpXP, which plays a role in modulating mutagenesis by degrading UmuD and UmuD′ as well as DinB (48,49). Furthermore, the UmuD G92D mutation is poorly cleavable, but when this mutation was constructed in the context of UmuD′, cells harboring this variant were mutable to a similar extent as cells harboring wild-type UmuD (50,51), suggesting that the G92D mutation does not alter the ability of UmuD′ to facilitate UmuC-dependent mutagenesis. On the other hand, the UmuD G92C variant was as proficient for cleavage as wild-type UmuD (52). Therefore, this region of UmuD seems to be an important site for a number of protein interactions.

The C-terminal domain of α facilitates numerous interactions necessary for efficient replication, as it interacts with the β clamp (30), ssDNA (31) and the τ subunit of the clamp loader (53,54). The interaction between α and the β clamp is essential for high processivity. However, as replication on the lagging strand is carried out in a series of Okazaki fragments that are synthesized in a discontinuous manner, the polymerase on the lagging strand must be recycled for each Okazaki fragment. Although the exact mechanism of the processivity switch is unknown, the OB fold of α has been implicated as a sensor for ssDNA such that when synthesis of an Okazaki fragment is completed, the affinity of α for the β clamp is decreased and α is released from the clamp and from DNA (55–57). Thus, the interaction between α and ssDNA is proposed to act as a processivity switch. In this work, we demonstrated that SOS-induced levels of UmuD inhibit binding of α to ssDNA. UmuD also inhibits binding of α to the β clamp, and these two mechanisms likely work together to facilitate polymerase exchange.

UmuD, together with UmuC, specifically decrease the rate of DNA replication and therefore were proposed to participate in a primitive DNA damage checkpoint

(21–23). We previously showed that UmuD, but not the cleaved form UmuD′, disrupts the binding of α to the β clamp, which provides a possible molecular explanation for the role of UmuD in a primitive checkpoint (29). The question then arises of the role of UmuD disruption of ssDNA binding by α. It has been shown that DNA damage on the lagging strand does not disrupt DNA replication, whereas DNA damage on the leading strand may severely disrupt replication or may cause leading strand replication to occur discontinuously, as the polymerase can re-initiate synthesis downstream of the damage (8–10). Polymerases that encounter DNA damage can also become stalled in a futile cycle of insertion and excision of nucleotides (58), as they fail to copy the damaged DNA. Our observations suggest that UmuD would then rescue the stalled polymerase by preventing α from binding to ssDNA or to the β clamp, thereby allowing DNA repair proteins or translesion DNA polymerases access to the damaged DNA.

Taken together, our findings suggest that UmuD specifically disrupts the interaction between α and ssDNA, inhibiting access to the ssDNA template by the replicative polymerase as part of the primitive DNA damage checkpoint to allow DNA repair. UmuD may also prevent binding of α to ssDNA to facilitate polymerase exchange, allowing an error-prone translesion synthesis polymerase to copy damaged DNA so that DNA replication may proceed. Our results demonstrate a new mechanism by which UmuD may regulate the cellular response to DNA damage.

REFERENCES

1. Johnson,A. and O'Donnell,M. (2005) Cellular DNA replicases: components and dynamics at the replication fork. *Annu. Rev. Biochem.*, **74**, 283–315.

2. Kelman,Z. and O'Donnell,M. (1995) DNA polymerase III holoenzyme: structure and function of a chromosomal replicating machine. *Annu. Rev. Biochem.*, **64**, 171–200.
3. Conte,E., Vincelli,G., Schaaper,R.M., Bressanin,D., Stefan,A., Dal Piaz,F. and Hochkoeppler,A. (2012) Stabilization of the *Escherichia coli* DNA polymerase III epsilon subunit by the theta subunit favors *in vivo* assembly of the Pol III catalytic core. *Arch. Biochem. Biophys.*, **523**, 135–143.
4. Taft-Benz,S.A. and Schaaper,R.M. (2004) The theta subunit of *Escherichia coli* DNA polymerase III: a role in stabilizing the epsilon proofreading subunit. *J. Bacteriol.*, **186**, 2774–2780.
5. Ellison,V. and Stillman,B. (2001) Opening of the clamp: an intimate view of an ATP-driven biological machine. *Cell*, **106**, 655–660.
6. Gao,D.X. and McHenry,C.S. (2001) Tau binds and organizes *Escherichia coli* replication proteins through distinct domains: partial proteolysis of terminally tagged tau to determine candidate domains and to assign domain V as the alpha binding domain. *J. Biol. Chem.*, **276**, 4433–4440.
7. Clover,B.P. and McHenry,C.S. (2001) The DNA polymerase III holoenzyme: an asymmetric dimeric replicative complex with leading and lagging strand polymerases. *Cell*, **105**, 925–934.
8. Higuchi,K., Katayama,T., Iwai,S., Hidaka,M., Horiuchi,T. and Maki,H. (2003) Fate of DNA replication fork encountering a single DNA lesion during oriC plasmid DNA replication *in vitro*. *Genes Cells*, **8**, 437–449.
9. Pages,V. and Fuchs,R.P. (2003) Uncoupling of leading- and lagging-strand DNA replication during lesion bypass *in vivo*. *Science*, **300**, 1300–1303.
10. Yeeles,J.T.P. and Marians,K.J. (2011) The *Escherichia coli* replisome is inherently DNA damage tolerant. *Science*, **334**, 235–238.
11. Fujii,S. and Fuchs,R.P. (2007) Interplay among replicative and specialized DNA polymerases determines failure or success of translesion synthesis pathways. *J. Mol. Biol.*, **372**, 883–893.
12. Sassanfar,M. and Roberts,J.W. (1990) Nature of the SOS-inducing signal in *Escherichia coli*: the involvement of DNA replication. *J. Mol. Biol.*, **212**, 79–96.
13. Simmons,L.A., Foti,J.J., Cohen,S.E. and Walker,G.C. (2008) In: Bock,A., Curtiss,R. III, Kaper,J.B., Karp,P.D., Neidhardt,F.C., Nystrom,T., Slauch,J.M., Squires,C.L. and Ussary,D. (eds), *Escherichia coli and Salmonella: Cellular and Molecular Biology*. ASM Press, Washington, D.C.
14. Reuven,N.B., Arad,G., Maor-Shoshani,A. and Livneh,Z. (1999) The mutagenesis protein UmuC is a DNA polymerase activated by UmuD′, RecA, and SSB and is specialized for translesion replication. *J. Biol. Chem.*, **274**, 31763–31766.
15. Tang,M., Shen,X., Frank,E.G., O'Donnell,M., Woodgate,R. and Goodman,M.F. (1999) UmuD′2C is an error-prone DNA polymerase, *Escherichia coli* pol V. *Proc. Natl Acad. Sci. USA*, **96**, 8919–8924.
16. Wagner,J., Gruz,P., Kim,S.R., Yamada,M., Matsui,K., Fuchs,R.P.P. and Nohmi,T. (1999) The *dinB* gene encodes a novel *E. coli* DNA polymerase, DNA pol IV, involved in mutagenesis. *Mol. Cell*, **4**, 281–286.
17. Jarosz,D.F., Beuning,P.J., Cohen,S.E. and Walker,G.C. (2007) Y-family DNA polymerases in *Escherichia coli*. *Trends Microbiol.*, **15**, 70–77.
18. Yang,W. and Woodgate,R. (2007) What a difference a decade makes: insights into translesion DNA synthesis. *Proc. Natl Acad. Sci. USA*, **104**, 15591–15598.
19. Pata,J.D. (2010) Structural diversity of the Y-family DNA polymerases. *Biochim. Biophys. Acta*, **1804**, 1124–1135.
20. Washington,M.T., Carlson,K.D., Freudenthal,B.D. and Pryor,J.M. (2010) Variations on a theme: Eukaryotic Y-family DNA polymerases. *Biochim. Biophys. Acta*, **1804**, 1113–1123.
21. Marsh,L. and Walker,G.C. (1985) Cold sensitivity induced by overproduction of UmuDC in *Escherichia coli*. *J. Bacteriol.*, **162**, 155–161.
22. Opperman,T., Murli,S., Smith,B.T. and Walker,G.C. (1999) A model for a *umuDC*-dependent prokaryotic DNA damage checkpoint. *Proc. Natl Acad. Sci. USA*, **96**, 9218–9223.
23. Sutton,M.D. and Walker,G.C. (2001) *umuDC*-mediated cold sensitivity is a manifestation of functions of the UmuD2C complex involved in a DNA damage checkpoint control. *J. Bacteriol.*, **183**, 1215–1224.
24. Ollivierre,J.N., Fang,J. and Beuning,P.J. (2010) The roles of UmuD in regulating mutagenesis. *J. Nucleic Acids*, **2010**, pii: 947680.
25. Simon,S.M., Sousa,F.J., Mohana-Borges,R. and Walker,G.C. (2008) Regulation of *Escherichia coli* SOS mutagenesis by dimeric intrinsically disordered *umuD* gene products. *Proc. Natl Acad. Sci. USA*, **105**, 1152–1157.
26. Godoy,V.G., Jarosz,D.F., Simon,S.M., Abyzov,A., Ilyin,V. and Walker,G.C. (2007) UmuD and RecA directly modulate the mutagenic potential of the Y family DNA polymerase DinB. *Mol. Cell*, **28**, 1058–1070.
27. Rajagopalan,M., Lu,C., Woodgate,R., O'Donnell,M., Goodman,M.F. and Echols,H. (1992) Activity of the purified mutagenesis proteins UmuC, UmuD′, and RecA in replicative bypass of an abasic DNA lesion by DNA polymerase III. *Proc. Natl Acad. Sci. USA*, **89**, 10777–10781.
28. Sutton,M.D., Opperman,T. and Walker,G.C. (1999) The *Escherichia coli* SOS mutagenesis proteins UmuD and UmuD′ interact physically with the replicative DNA polymerase. *Proc. Natl Acad. Sci. USA*, **96**, 12373–12378.
29. Silva,M.C., Nevin,P., Ronayne,E.A. and Beuning,P.J. (2012) Selective disruption of the DNA polymerase III alpha-beta complex by the umuD gene products. *Nucleic Acids Res.*, **40**, 5511–5522.
30. Dohrmann,P.R. and McHenry,C.S. (2005) A bipartite polymerase-processivity factor interaction: Only the internal beta binding site of the alpha subunit is required for processive replication by the DNA polymerase III holoenzyme. *J. Mol. Biol.*, **350**, 228–239.
31. McCauley,M.J., Shokri,L., Sefcikova,J., Venclovas,C., Beuning,P.J. and Williams,M.C. (2008) Distinct double- and single-stranded DNA binding of *E. coli* replicative DNA polymerase III alpha subunit. *ACS Chem. Biol.*, **3**, 577–587.
32. Beuning,P.J., Simon,S.M., Godoy,V.G., Jarosz,D.F. and Walker,G.C. (2006) Characterization of *Escherichia coli* translesion synthesis polymerases and their accessory factors. *Methods Enzymol.*, **408**, 318–340.
33. Beuning,P.J., Simon,S.M., Zemla,A., Barsky,D. and Walker,G.C. (2006) A non-cleavable UmuD variant that acts as a UmuD′ mimic. *J. Biol. Chem.*, **281**, 9633–9640.
34. Chaurasiya,K.R., Paramanathan,T., McCauley,M.J. and Williams,M.C. (2010) Biophysical characterization of DNA binding from single molecule force measurements. *Phys. Life Rev.*, **7**, 299–341.
35. Vladescu,I.D., McCauley,M.J., Rouzina,I. and Williams,M.C. (2005) Mapping the phase diagram of single DNA molecule force-induced melting in the presence of ethidium. *Phys. Rev. Lett.*, **95**, 158102.
36. Sharma,R. (2010) *M.S. Thesis*. Northeastern University, Boston, MA.
37. Kozakov,D., Hall,D.R., Beglov,D., Brenke,R., Comeau,S.R., Shen,Y., Li,K., Zheng,J., Vakili,P., Paschalidis,I. *et al.* (2010) Achieving reliability and high accuracy in automated protein docking: ClusPro, PIPER, SDU, and stability analysis in CAPRI rounds 13-19. *Proteins*, **78**, 3124–3130.
38. Kozakov,D., Brenke,R., Comeau,S.R. and Vajda,S. (2006) PIPER: an FFT-based protein docking program with pairwise potentials. *Proteins*, **65**, 392–406.
39. Comeau,S.R., Gatchell,D.W., Vajda,S. and Camacho,C.J. (2004) ClusPro: a fully automated algorithm for protein-protein docking. *Nucleic Acids Res.*, **32**, W96–W99.
40. Comeau,S.R., Gatchell,D.W., Vajda,S. and Camacho,C.J. (2004) ClusPro: an automated docking and discrimination method for the prediction of protein complexes. *Bioinformatics*, **20**, 45–50.
41. Tovchigrechko,A. and Vakser,I.A. (2006) GRAMM-X public web server for protein-protein docking. *Nucleic Acids Res.*, **34**, W310–W314.
42. Schneidman-Duhovny,D., Inbar,Y., Nussinov,R. and Wolfson,H.J. (2005) PatchDock and SymmDock: servers for rigid and symmetric docking. *Nucleic Acids Res.*, **33**, W363–W367.
43. Lyskov,S. and Gray,J.J. (2008) The RosettaDock server for local protein-protein docking. *Nucleic Acids Res.*, **36**, W233–W238.

44. Ericsson,U.B., Hallberg,B.M., Detitta,G.T., Dekker,N. and Nordlund,P. (2006) Thermofluor-based high-throughput stability optimization of proteins for structural studies. *Anal. Biochem.*, **357**, 289–298.

45. Shokri,L., McCauley,M.J., Rouzina,I. and Williams,M.C. (2008) DNA overstretching in the presence of glyoxal: structural evidence of force-induced DNA melting. *Biophys. J.*, **95**, 1248–1255.

46. Fang,J., Rand,K.D., Silva,M.C., Wales,T.E., Engen,J.R. and Beuning,P.J. (2010) Conformational dynamics of the *Escherichia coli* DNA polymerase manager proteins UmuD and UmuD′. *J. Mol. Biol.*, **398**, 40–53.

47. Woodgate,R. and Ennis,D.G. (1991) Levels of chromosomally encoded Umu proteins and requirements for *in vivo* UmuD cleavage. *Mol. Gen. Genet.*, **229**, 10–16.

48. Amar,A., Al Mamun,M. and Humayun,M.Z. (2009) Spontaneous mutagenesis is elevated in protease-defective cells. *Mol. Microbiol.*, **71**, 629–639.

49. Neher,S.B., Sauer,R.T. and Baker,T.A. (2003) Distinct peptide signals in the UmuD and UmuD′ subunits of UmuD/D′ mediate tethering and substrate processing by the ClpXP protease. *Proc. Natl Acad. Sci. USA*, **100**, 13219–13224.

50. McLenigan,M., Peat,T.S., Frank,E.G., McDonald,J.P., Gonzalez,M., Levine,A.S., Hendrickson,W.A. and Woodgate,R. (1998) Novel *Escherichia coli umuD′* mutants: structure-function insights into SOS mutagenesis. *J. Bacteriol.*, **180**, 4658–4666.

51. Battista,J.R., Ohta,T., Nohmi,T., Sun,W. and Walker,G.C. (1990) Dominant negative *umuD* mutations decreasing RecA-mediated cleavage suggest roles for intact UmuD in modulation of SOS mutagenesis. *Proc. Natl Acad. Sci. USA*, **87**, 7190–7194.

52. Ollivierre,J.N., Sikora,J.L. and Beuning,P.J. (2013) Dimer exchange and cleavage specificity of the DNA damage response protein UmuD. *Biochim. Biophys. Acta*, **1834**, 611–620.

53. Kim,D.R. and McHenry,C.S. (1996) Biotin tagging deletion analysis of domain limits involved in protein-macromolecular interactions: mapping the tau binding domain of the DNA polymerase III alpha subunit. *J. Biol. Chem.*, **271**, 20690–20698.

54. Jergic,S., Ozawa,K., Williams,N.K., Su,X.C., Scott,D.D., Hamdan,S.M., Crowther,J.A., Otting,G. and Dixon,N.E. (2007) The unstructured C-terminus of the tau subunit of *Escherichia coli* DNA polymerase III holoenzyme is the site of interaction with the alpha subunit. *Nucleic Acids Res.*, **35**, 2813–2824.

55. Dohrmann,P.R., Manhart,C.M., Downey,C.D. and McHenry,C.S. (2011) The rate of polymerase release upon filling the gap between Okazaki fragments is inadequate to support cycling during lagging strand synthesis. *J. Mol. Biol.*, **414**, 15–27.

56. Georgescu,R.E., Kurth,I., Yao,N.Y., Stewart,J., Yurieva,O. and O'Donnell,M. (2009) Mechanism of polymerase collision release from sliding clamps on the lagging strand. *EMBO J.*, **28**, 2981–2991.

57. Kurth,I., Georgescu,R.E. and O'Donnell,M.E. (2013) A solution to release twisted DNA during chromosome replication by coupled DNA polymerases. *Nature*, **496**, 119–122.

58. Pages,V., Janel-Bintz,R. and Fuchs,R.P. (2005) Pol III proofreading activity prevents lesion bypass as evidenced by its molecular signature within *E. coli* cells. *J. Mol. Biol.*, **352**, 501–509.